Wireless Pers Commun
https://doi.org/10.1007/s11277-017-5123-1

High Performance Microstrip Low Pass Filter for Wireless Communications

Saeed Roshani[1] · Alireza Golestanifar[2] · Amirhossein Ghaderi[2] · Hesam Siahkamari[2] · Derek Abbott[3]

Abstract A microstrip low-pass filter using T-shaped resonators is designed to achieve an ultra-sharp transition band and high suppression level. The performance of the resonators is investigated based on an LC equivalent circuit and a transfer function to compute the equations of the transmission zeros. This filter has an acceptable stopband with high insertion loss (28 dB) by adopting a rectangular suppressor. Also, the width of the transition band is 0.09 GHz (with – 3 and – 40 dB attenuation levels), that exhibits a very high sharpness ($\xi = 411$ dB/GHz). The proposed filter with a 3 dB cut-off frequency (f_c) of 1.32 GHz presents a high return loss in the passband (17 dB) and high figure of merit of 57,073. The designed filter is fabricated and measured, demonstrating sufficient agreement between the simulation and experimental results.

Keywords T-shaped resonator · LC equivalent circuit · Microstrip filter · Rectangular stub

1 Introduction

To reject unwanted signals, microstrip LPFs with high insertion loss in the stopband, sharp cut-off and low cost are utilized in wireless circuits [1]. In [2], a hairpin LPF with high return loss in the passband was presented; nonetheless the sharpness of the transition band is poor. In [3], a novel LPF using multi-mode resonators was reported. For increasing the stopband width, two small multi-mode stubs were utilized; however, slow cut-off

✉ Saeed Roshani
s_roshany@yahoo.com

[1] Department of Electrical Engineering, Kermanshah Branch, Islamic Azad University, Kermanshah, Iran

[2] Young Researchers and Elite Club, Kermanshah Branch, Islamic Azad University, Kermanshah, Iran

[3] School of Electrical and Electronic Engineering, University of Adelaide, Adelaide, Australia

Published online: 14 December 2017

frequency, low insertion loss in the stopband and low return loss in the passband are undesired features of this work. In [4], a hairpin filter with small dimensions was studied. Slow transition band and low suppression level are drawbacks of this work. A dual-layer LPF using a stepped-impedance resonator was presented in [5]. To expand the stopband width, a defected ground plane was added; nevertheless this filter does not have a sharp cut-off and has high insertion loss in the passband. In [6], an LPF using a dual-layer structure was fabricated. In this filter, a defected ground plane was adopted to approach a sharp transition band, although it suffers from a complex structure and weak sharpness. An LPF with low suppression level, complex structure and slow transition band was reported in [7]. By adopting several stepped-impedance stubs, an LPF with a simple topology was fabricated in [8]. Weak sharpness and enormous size are disadvantages of this filter. A hairpin LPF with large size and weak sharpness in the passband was designed in [9]. To extend the stopband width, two hairpin resonators was cascaded in this filter. In [10], a microstrip LPF using dual-plane structure was reported that it have a weak harmonic suppression under − 20 dB suppression level and slow cut-off frequency. An LPF with high suppression level in the stopband area using an spiral transmission line and stepped-impedance stubs was introduced in [11]. In [12], an LPF with small dimensions and simple topology using stepped-impedance structures was designed that its cut-off frequency is not so sharp. A microstrip filter using dual plane structure was fabricated in [13]. High return loss and sharp transition-band are benefits of this work. A dual-layer LPF using open-circuited stubs was presented in [14], unfortunately it suffers from complex structure, large size and weak sharpness. In [15–17], dual-plane LPFs were designed that they do not have a sharp cut-off frequency and small dimensions. A symmetrical LPF using P-shaped and Lattice-Shaped resonators was introduced in [18]. Although the return loss in the passband is high, the dimensions of this filter are very large. In [19, 20], slow transition-band is the greatest problem of these LPFs. In [21], to increase the stopband width, stepped-impedance stubs are adopted at the beginning and end of transmission line; however, the sharpness of transition-band is weak. In [22], for achieving a compact size, an spiral transmission line was utilized. Also, the limited stopband and weak sharpness are problems of this circuit.

In this work, a low-pass filter with high return loss in the passband and ultra-sharp transition band is presented. This filter is composed of T-shaped resonators and one rectangular stub as a suppressing unit. Also, to achieve a compact size, this structure is bent.

2 Design Process

2.1 T-Shaped Resonator

Figure 1a exhibits a T-shaped resonator composed of a high impedance stub and one rectangular open-circuited stub, which they are connected to the transmission line. The LC equivalent circuit of this resonator is presented in Fig. 1b. The transmission line with L_1, L_2 and C_1 is modelled as inductances and capacitance, respectively. L_3 and C_2 exhibit the inductance and capacitance of the high-impedance stub and L_4 and C_3 are equivalent inductance and capacitance of the open-circuited stub. The values of the lumped elements using equations cited in [1] are computed and they are as follows: $L_1 = 16.34$ nH, $L_2 = 5.21$ nH, $L_3 = 10.22$ nH, $L_4 = 1.164$ nH, $C_1 = 1.11$ pF, $C_2 = 0.22$ pF and $C_3 = 0.96$ pF. The EM and LC simulation results of the T-shaped resonator are depicted in

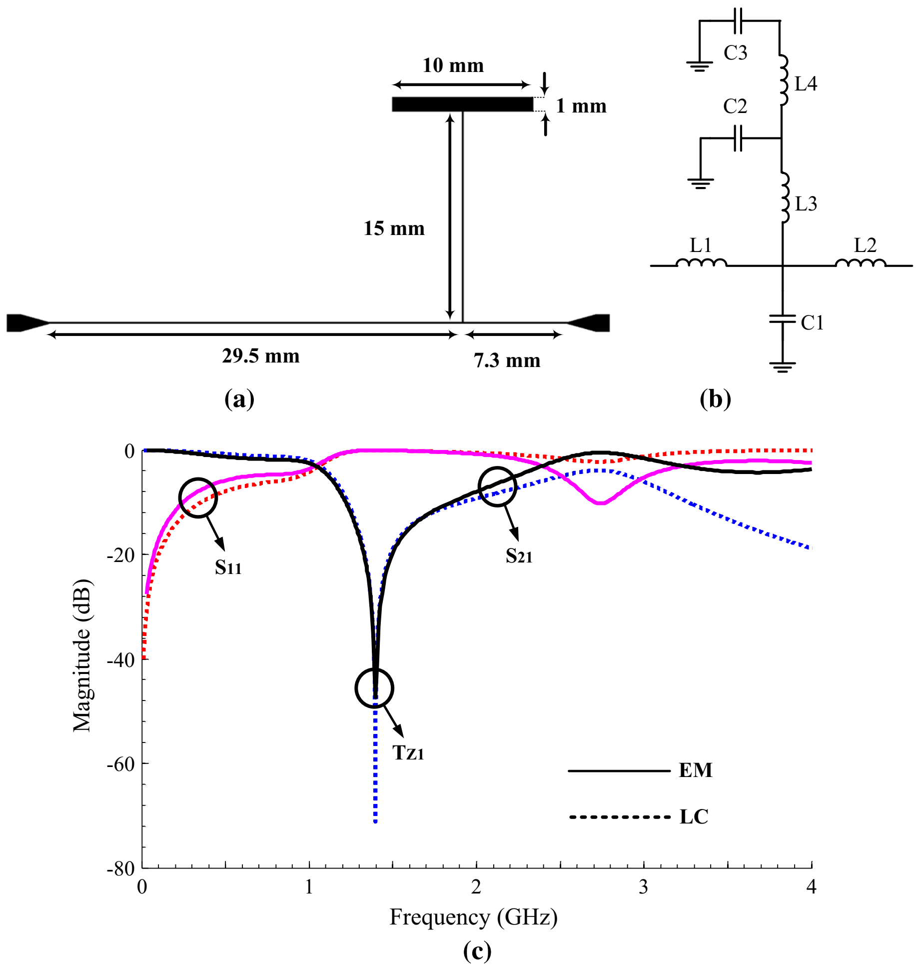

Fig. 1 T-shaped resonator: **a** layout, **b** LC equivalent circuit, **c** EM and LC simulations

Fig. 1c. As seen, this structure has a sharp transition band and produces a transmission zero (TZ_1) at 1.4 GHz, that transition band is tuned by it. To obtain the equation of the TZ_1, the transfer function is presented in Eq. (1), that r is the matching impedance of input and output ports (r = 50 Ω). Here, TZ_1 is calculated by equalling numerator of transfer function with zero in Eq. (2).

$$\frac{V_o}{V_i} = \frac{2r}{L_2S(L_1C_1S^2 + b + 1) + r(L_1C_1S^2 + aL_2S + b + 2) + r^2a + L_1S}, \quad (1)$$

where

$$a = \frac{C_2C_3L_4S^3 + (C_2 + C_3)S}{C_2C_3L_4L_3S^4 + (C_2L_3 + C_3L_3 + C_3L_4)S^2 + 1} + C_1S,$$

$$b = \frac{L_1 S(C_2 C_3 L_4 S^3 + (C_2 + C_3)S)}{C_2 C_3 L_4 L_3 S^4 + (C_2 L_3 + C_3 L_3 + C_3 L_4)S^2 + 1}.$$

$$T_{Z1} = \frac{1}{2\pi\sqrt{(C_2 C_3 L_4 L_3) + (C_2 L_3 + C_3 L_3 + C_3 L_4)}}. \quad (2)$$

2.2 Dual T-Shaped Resonator

The layout of the dual T-shaped resonator is illustrated in Fig. 2a. This resonator with shunt capacitors and series inductors is modelled in Fig. 2b. The values of the LC equivalent circuit are as follows: $L_5 = 10.78$ nH, $L_6 = 6.036$ nH, $L_7 = 0.156$ nH, $C_4 = 0.5$ pF, $C_5 = 0.71$ pF, $C_6 = 0.4$ pF and $C_7 = 0.966$ pF. The EM and LC simulation results are depicted in Fig. 2c. This structure can improve the suppression level by producing a transmission zero (TZ_2) at 1.78 GHz. The transfer function of the dual T-shaped

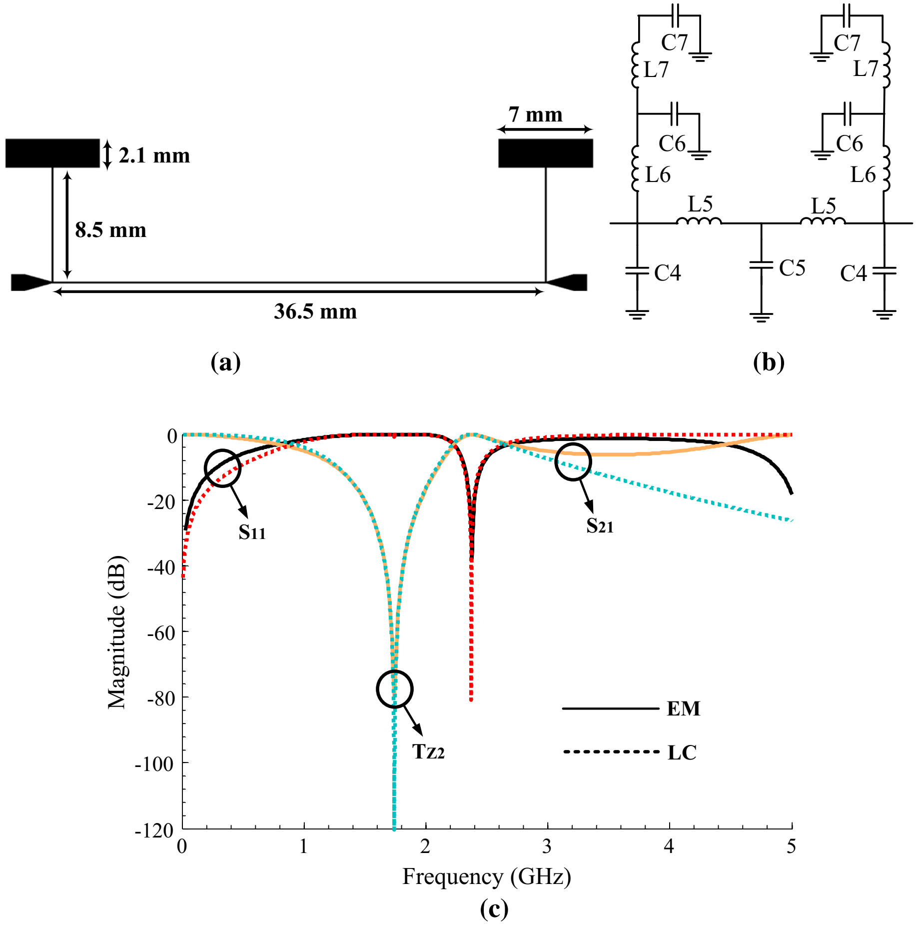

Fig. 2 Dual T-shaped resonator: **a** layout, **b** LC equivalent circuit, **c** EM and LC simulations

resonator is displayed in Eq. (3). Also, the equation of the TZ_2 is obtained from Eq. (3) and shown in Eq. (4).

$$\frac{V_o}{V_{in}} = \frac{2Z_0d}{\begin{array}{c} dL_5S + dL_5S(C_5L_5S^2+1) + Z_0^2c + Z_0^2(a+b+1)c + dZ_0^2C_5S(b+1) \\ + Z_0da + Z_0dC_5L_5S^2 + Z_0(L_5S + L_5S(C_5L_5S^2+1))c + Z_0db + 2Z_0d \end{array}}, \quad (3)$$

where

$$a = L_5S\left(\frac{c}{d} + C_5S(b+1)\right),$$

$$b = \frac{cL_5S}{d},$$

$$c = C_4C_6C_7L_7L_6S^5 + (C_4C_6L_6 + C_4C_7L_6 + C_4C_7L_7 + C_6C_7L_7)S^3 + (C_4 + C_6 + C_7)S,$$

$$d = (C_6C_7L_7L_6S^4 + (C_6L_6 + C_7L_6 + C_7L_7)S^2 + 1).$$

$$T_{Z2} = \frac{1}{2\pi\sqrt{(C_6C_7L_6L_7) + (C_6L_6 + C_7L_6 + C_7L_7)}}. \quad (4)$$

2.3 Rectangular Resonator

The layout and LC equivalent circuit of rectangular resonator are displayed in Fig. 3a, b. In this model, L_8, L_9 and C_8 are inductances and capacitance of transmission line. Also, L_{10} and C_9 denote inductance and capacitance of rectangular stub. The values of these parameters are as follows: $L_8 = 9.6$ nH, $L_9 = 12$ nH, $L_{10} = 2.41$ nH, $C_8 = 3.7$ pF and $C_9 = 0.49$ pF. Figure 3c shows EM and LC simulation results of this structure. As seen, this circuit generates a transmission zero (TZ_3) at 4.6 GHz that to compute the equation of TZ_3, the transfer function of rectangular stub is achieved from its LC equivalent circuit. The transfer function and equation of TZ_3 are presented in Eqs. (5) and (6), respectively.

$$\frac{V_o}{V_{in}} = \frac{2Z_0(C_9L_{10}S^2+1)}{\begin{array}{c} L_8S(C_9L_{10}S^2+1) + aL_9L_8S^2 + L_9S(C_9L_{10}S^2+1) + aZ_0^2 \\ + (aZ_0L_8 + aZ_0L_9)S + 2Z_0(C_9L_{10}S^2+1) \end{array}}, \quad (5)$$

where

$$a = C_8S + C_9S + C_9C_8L_{10}S^3.$$

$$T_{Z3} = \frac{1}{2\pi\sqrt{C_9L_{10}}}. \quad (6)$$

2.4 LPF Design

To design a high performance low-pass filter, T-shaped resonators and rectangular stub (as suppressing unit) are combined, as depicted in Fig. 4a. The primitive LPF has an acceptable stopband with high insertion loss and sharp cut-off frequency (seen in Fig. 4b), but the circuit dimensions are large. Ho wever, we have achieved a compact layout, as seen

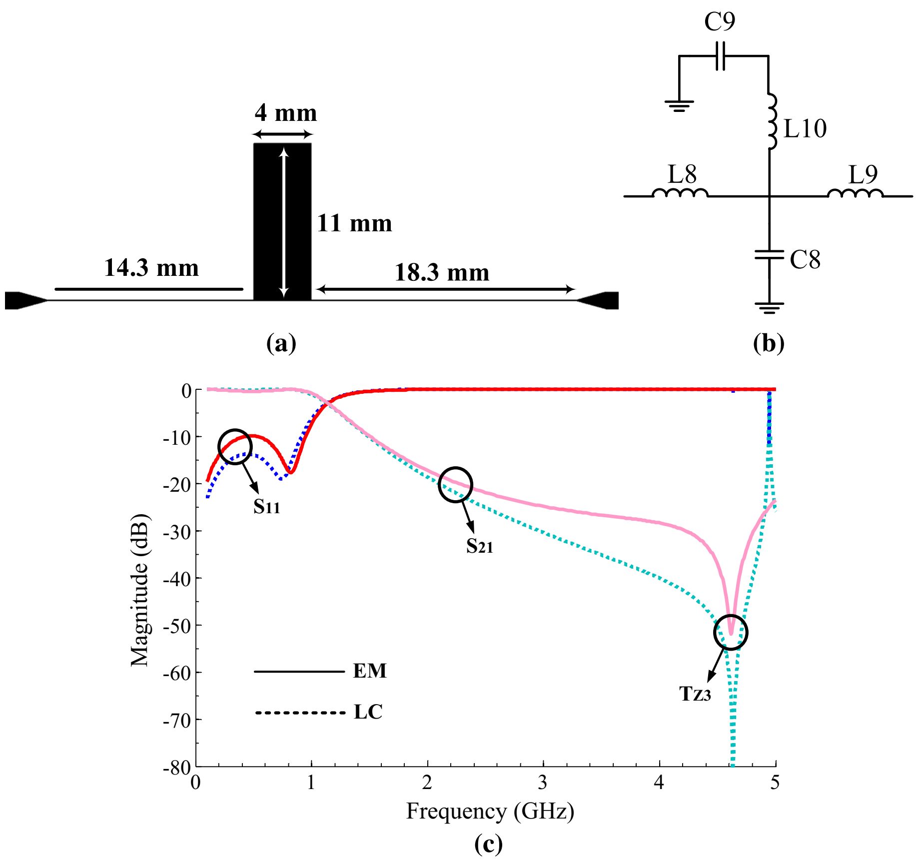

Fig. 3 Rectangular resonator: **a** layout, **b** LC equivalent circuit, **c** EM and LC simulations

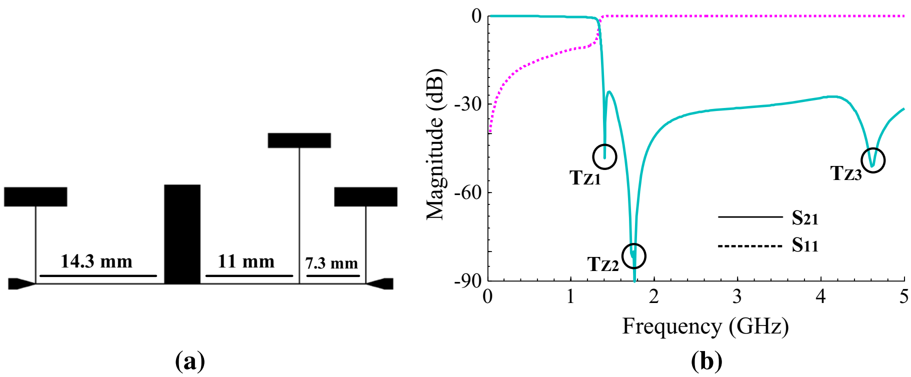

Fig. 4 Primitive LPF: **a** layout, **b** EM simulation

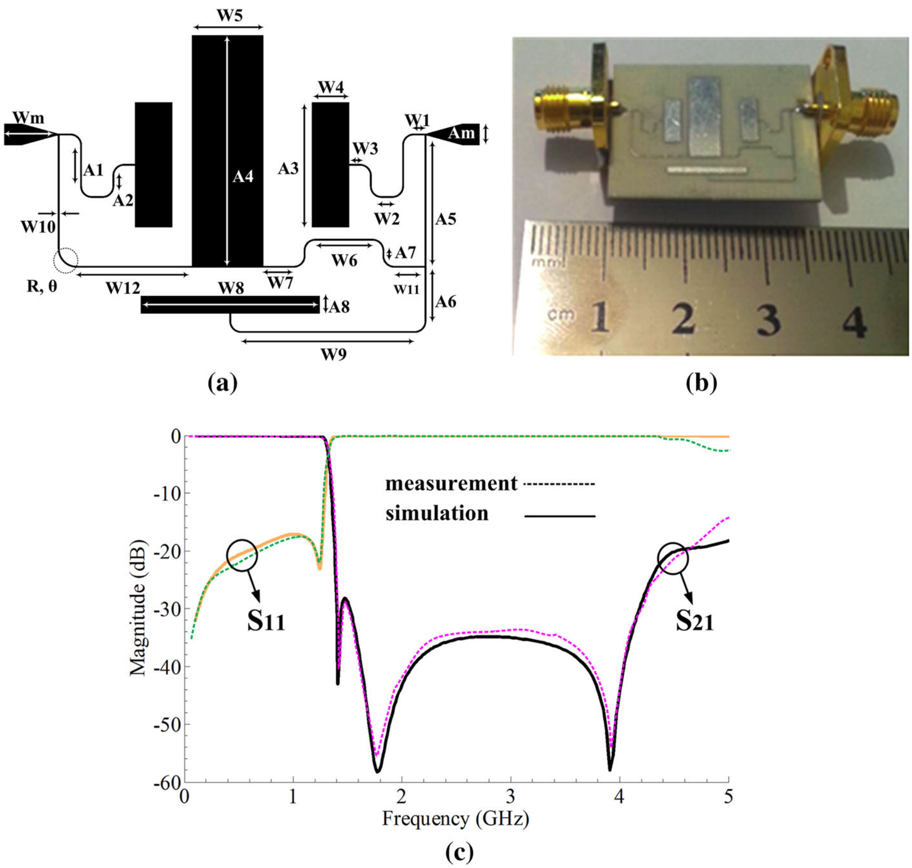

Fig. 5 Proposed LPF: **a** layout, **b** fabricated photo, **c** simulation and measurement results

in Fig. 5a. The proposed filter shows 44% size reduction in comparison with previous structure.

3 Simulated and Measured Results

The proposed filter with 3 dB cut-off frequency of 1.32 GHz is fabricated on a substrate (Rogers_RO4003) with $\varepsilon_r = 3.38$, thickness = 0.508 mm and loss-tangent = 0.002 (As illustrated in Fig. 5b) and tested using an Agilent N5230A network analyser. The simulation results are taken by the ADS software. The simulation and measurement results are depicted in Fig. 5c.

The final LPF with high return loss (RL) in the passband (17 dB) has an ultra-sharp transition band ($\xi = 411$ dB/GHz) from 1.32 to 1.41 GHz (with − 3 and − 40 dB attenuation levels). The stopband with excellent suppression level (− 28 dB) is extended from 1.4 to 4.218 GHz (3.19 f_c).

The circuit dimensions are $0.158\lambda_g \times 0.128\lambda_g$, where λ_g is guided wave-length at f_c. Finally, the designed LPF presents a high FOM of 57,073. The physical dimensions of this

Table 1 Comparison among reported works and proposed one

References	ξ	SF	RSB	NCS	AF	FOM	RL
[2]	52.8	2	1.529	0.081 × 0.113	1	17,640	23
[3]	16.5	1.5	1.58	0.090 × 0.110	1	3950	10
[4]	95	2	1.4	0.104 × 0.214	1	7388	16
[5]	188	2	0.9	0.200 × 0.180	2	4700	10
[6]	162	2.5	1.124	–	2	–	15
[7]	256	1.5	1.574	0.148 × 0.157	1	38747	10
[13]	159	2	1.146	0.316 × 0.689	2	837	12.5
[17]	29.3	2.4	1.534	0.0075	2	7191.4	20
[18]	100	2	1.58	0.184 × 0.478	1	3593	19
[21]	94	2.3	1.262	0.244 × 0.169	1	6616.7	17
[22]	–	2	0.332	0.337 × 0.253	1	–	20
This work	411	2.8	1.003	0.158 × 0.128	1	57,073	17

filter are as follows: $A_1 = 2.3$, $A_2 = 0.6$, $A_3 = 7$, $A_4 = 13$, $A_5 = 7.3$, $A_6 = 3$, $A_7 = 0.31$, $A_8 = 1$, $A_m = 1.2$, $W_1 = 0.6$, $W_2 = 0.6$, $W_3 = 0.6$, $W_4 = 2.1$, $W_5 = 4$, $W_6 = 3.2$, $W_7 = 1.7$, $W_8 = 10$, $W_9 = 9.7$, $W_{10} = 0.1$, $W_{11} = 1.7$, $W_{12} = 6.43$, $W_m = 3$, $R = 1$ (all in millimeters) and $\theta = 90°$. The proposed filter and reported works are compared in Table 1 based on parameters outlined in [23, 24].

As shown in Table 1, our filter has the sharpest cut-off frequency, the highest suppression level and the highest FOM in comparison with published works in [2–6].Transition band sharpness (ξ) is for − 3 and − 40 dB suppression points. The table also lists the suppression factor (SF) and RSB is the relative stopband band-width. The normalized circuit size is given by NCS. AF is architecture facture and FOM is figure of merit [FOM = (ξ × RSB × SF)/(NCS × AF)].

4 Conclusion

A microstrip low-pass filter using T-shaped resonators (to approach sharp cut-off and high suppression level) and one rectangular stub (to increase the stopband width) has been designed, fabricated and tested. This filter presents excellent features like, simple topology, narrow transition band (0.09 GHz), high insertion loss in the stopband (28 dB), small dimensions and very high FOM of 57,073. The final structure with 3 dB cut-off frequency of 1.32 GHz is suitable for wireless communications.

Acknowledgements The authors would like to thank the Kermanshah Branch, Islamic Azad University for the financial support of this research project.

References

1. Hong, J. S., & Lancaster, M. J. (2001). *Microstrip filters for RF/microwave applications*. New York: Wiley.

2. Liu, S., Xu, J., & Xu, Z. (2014). Compact lowpass filter with wide stopband using stepped impedance hairpin units. *Electronics Letters, 51*(1), 67–69.
3. Li, Q., Zhang, Y., & Fan, Y. (2015). Compact ultra-wide stopband low pass filter using multimode resonators. *Electronics Letters, 51*(14), 1084–1085.
4. Velidi, V. K., & Sanyal, S. (2011). Sharp roll-off lowpass filter with wide stopband using stub-loaded coupled-line hairpin unit. *IEEE Microwave and Wireless Components Letters, 21*(6), 301–303.
5. Xiao, M., Sun, G., & Li, X. (2015). A lowpass filter with compact size and sharp roll-off. *IEEE Microwave and Wireless Components Letters, 25*(12), 790–792.
6. Liu, S., Xu, J., & Xu, Z. (2015). Sharp roll-off lowpass filter using interdigital DGS slot. *Electronics Letters, 51*(17), 1343–1345.
7. Wang, J. P., Ge, L., Guo, Y. X., & Wu, W. (2010). Miniaturised microstrip lowpass filter with broad stopband and sharp roll-off. *Electronics Letters, 46*(8), 573–575.
8. Asadbeigi, H., & Virdee, B. S. (2015). Compact notch filter design using stepped impedance resonators for sharp roll-off and large wideband rejection. *International Journal of RF and Microwave Computer-Aided Engineering, 25*(6), 490–494.
9. Li, L., Bao, J., Du, J. J., & Wang, Y. (2014). Stopband-extended and size-miniaturized low-pass filter with three transmission zeros. *ETRI Journal, 36*(2), 286–292.
10. Suhas, D., Lakshmi, C. R., Srinivasa Rao, Z., & Kannadassan, D. (2015). A systematic implementation of elliptic low-pass filters using defected ground structures. *Journal of Electromagnetic Waves and Applications, 29*(15), 2014–2026.
11. Khakzad, H. R., Sedighy, S. H., & Amirhosseini, M. K. (2013). Design of compact SITLs low pass filter by using invasive weed optimization (IWO) technique. *ACES Journal, 28*(3), 228–233.
12. Hayati, M., Shama, F., & Ekhteraei, M. (2016). Miniaturized microstrip suppressing cell with wide stopband. *Applied Computational Electromagnetics Society Journal, 31*(10), 1244–1249.
13. Zhang, P., & Li, M. (2016). A novel sharp roll-off microstrip lowpass filter with improved stopband and compact size using dual-plane structure. *Microwave and Optical Technology Letters, 58*(5), 1085–1088.
14. Kufa, M., & Raida, Z. (2013). Lowpass filter with reduced fractal defected ground structure. *Electronics Letters, 49*(3), 199–201.
15. Verma, A. K., Chaudhari, N. P., & Kumar, A. (2013). High performance microstrip transverse resonance lowpass filter. *Microwave and Optical Technology Letters, 55*(5), 1149–1152.
16. Boutejdar, A., Omar, A., & Burte, E. (2014). High-performance wide stop band low-pass filter using a vertically coupled DGS-DMS-resonators and interdigital capacitor. *Microwave and Optical Technology Letters, 56*(1), 87–91.
17. Majidifar, S. (2016). Design of high performance miniaturized lowpass filter using new approach of modeling. *Applied Computational Electromagnetics Society Journal, 31*(1), 52–57.
18. Hayati, M., Ekhteraei, M., & Shama, F. (2017). Compact lowpass filter with flat group delay using lattice-shaped resonator. *Electronics Letters, 53*(7), 475–476.
19. Kumar Singh, P., Kumar Tiwary, A., & Gupta, N. (2017). Ultra-compact switchable microstrip bandpass filter–low-pass filter with improved characteristics. *Microwave and Optical Technology Letters, 59*(1), 197–201.
20. Chen, X., Zhang, L., Peng, Y., Leng, Y., Lu, H., & Zheng, Z. (2015). Compact lowpass filter with wide stopband bandwidth. *Microwave and Optical Technology Letters, 57*(2), 367–371.
21. Raphika, P. M., Abdulla, P., & Jasmine, P. M. (2016). Planar elliptic function lowpass filter with sharp roll-off and wide stopband. *Microwave and Optical Technology Letters, 58*(1), 133–136.
22. Boutejdar, A. (2016). Design of a very compact U-HI-LO low-pass filter using meander technique and quasi horn inductors for L-band and C-band applications. *Microwave and Optical Technology Letters, 58*(12), 2897–2901.
23. Roshani, S. (2017). A compact microstrip low-pass filter with ultra wide stopband using compact microstrip resonant cells. *International Journal of Microwave and Wireless Technologies, 9*(5), 1023–1027.
24. Roshani, S., Golestanifar, A. R., Ghaderi, A. H., & Roshani, S. (2017). Miniaturized LPF with sharp transition-band using semi-circle resonators. *Applied Computational Electromagnetics Society Journal, 32*(4), 344–351.

Saeed Roshani received the B.Sc. degree in Electrical Engineering from Razi University, Kermanshah, Iran in 2008, M.Sc. degree in Electrical Engineering from Shahed University, Tehran, Iran in 2011 and Ph.D. in Electrical Engineering from Razi University in 2015. He performed opportunity research program in Amirkabir University of Technology (Tehran Polytechnics) Iran, in 2014–2015. He graduated as the best student of his country among all students of Iran on 2015 and Awarded by the First Vice President and science, research and technology Minister. He is currently an Assistant Professor in the Department of electrical engineering at Islamic Azad University, Kermanshah, Iran. He has published more than 40 papers in ISI Journals and Conferences and two books. His research interest includes the microwave and millimeter wave devices and circuits, low-power and low-size integrated circuit design.

Alireza Golestanifar was born in Kermanshah, Iran in 1993. He received his B.Sc. and M.Sc. degrees in Electronics Engineering from Islamic Azad University, Kermanshah, Iran in 2015 and 2017, respectively. He joined Young Researchers and Elite Club in 2017. His current research includes microwave passive circuits and RF integrated circuit design.

Amirhossein Ghaderi was born in Kermanshah, Iran in 1992. He received his B.Sc. and M.Sc. degrees in Electronics Engineering from Islamic Azad University, Kermanshah, Iran in 2015 and 2017, respectively (Honor). He selected as the best student in the Electronics Engineering Department and awarded by university president of Islamic Azad University, Kermanshah, Iran in 2014. He joined Young Researchers and Elite Club in 2017. His current research includes microwave passive circuits and RF integrated circuit design.

Hesam Siahkamari was born in Kermanshah, Iran in 1988. He received his B.Sc. degree in Electronic Engineering in 2010 from Islamic Azad University, Kermanshah, Iran and M.Sc. degree in Electronic Engineering in 2013 from Razi University, Kermanshah, Iran. His current research interest includes RF/microwave circuit design.

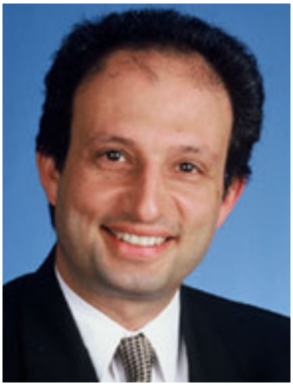

Derek Abbott was born in South Kensington, London, U.K., in 1960. He received the B.Sc. (honors) degree in physics from Lough borough University, Leicestershire, U.K., in 1982 and the Ph.D. degree in electrical and electronic engineering from The University of Adelaide, Adelaide, S.A. Australia, in 1995, under K. Eshraghian and B.R. Davis. From 1978 to 1986, he was a Research Engineer at the GEC Hirst Research Centre, London, U.K. From 1986 to 1987, he was a VLSI Design Engineer at Austek Microsystems, Australia. Since 1987, he has been with The University of Adelaide, where he is presently a full Professor with the School of Electrical and Electronic Engineering. He coedited Quantum Aspects of Life (London, U.K.: Imperial College Press, 2008), coauthored Stochastic Resonance (Cambridge, U.K.: Cambridge University Press, 2012), and coauthored Terahertz Imaging for Biomedical Applications (New York, NY, USA: Springer-Verlag, 2012). He holds over 800 publications/patents and has been an invited speaker at over 100 institutions. His interests are in the area of multidisciplinary physics and electronic engineering applied to complex systems. His research programs span a number of areas of stochastics, game theory, photonics, biomedical engineering, and computation al neuroscience. He is a Fellow of the Institute of Physics (IOP) and a Fellow of the IEEE. He has won a number of awards including the South Australian Tall Poppy Award for Science (2004), the Premier's SA Great Award in Science and Technology for outstanding contributions to South Australia (2004), and an Australian Research Council (ARC) Future Fellowship (2012). With his colleagues, he won an IEEE Sensors Journal best paper award (2014). He has served as an Editor and/or Guest Editor for a number of journals including the IEEE Journal of Solid-State Circuits, Journal of Optics B, the Microelectronics Journal, Chaos, Smart Structures and Materials, Fluctuation and Noise Letters, PLOSONE, and is currently on the editorial boards of the Proceedings of the IEEE, the IEEE Photonics Journal, and Nature's Scientific Reports.